Geophysical Survey at the early Christian complex of Son Peretó (Mallorca, Balearic Islands, Spain)

Journal:	*Archaeological Prospection*
Manuscript ID	ARP-20-0009.R1
Wiley - Manuscript type:	Research Article
Date Submitted by the Author:	n/a
Complete List of Authors:	Mas Florit, Catalina; Universitat de Barcelona, History and Archaeology Cau Ontiveros, Miguel Angel; Institucio Catalana de Recerca i Estudis Avancats, ; Universitat de Barcelona, Història i Arqueologia Meyer, Cornelius; cmprospection Sala, Roger; SOT Archaeological Prospection, Ortiz Quintana, Helena; SOT Prospecció Rodriguez Simón, Pedro; SOT Prospecció
Keywords:	Christianity, landscape, geophysics, magnetometry, GPR, church

Geophysical Survey at the early Christian complex of Son Peretó (Mallorca, Balearic Islands, Spain)

Authors:

Catalina Mas Florit*, Equip de Recerca Arqueològica i Arqueomètrica de la Universitat de Barcelona (ERAAUB), Spain

Miguel Ángel Cau Ontiveros**, ICREA, Pg. Lluís Companys 23, 08010 Barcelona, Spain; Equip de Recerca Arqueològica i Arqueomètrica de la Universitat de Barcelona (ERAAUB), Spain; Chercheur associé, Aix-Marseille Univ, CNRS, Centre Camille Jullian, Aix-en-Provence, France.

Cornelius Meyer, cmp Cornelius Meyer Prospection, Berlin, Germany

Roger Sala, SOT Prospecció arqueològica, Barcelona, Spain

Helena Ortiz-Quintana, SOT Prospecció arqueològica, Barcelona, Spain

Pedro Rodríguez Simón, SOT Prospecció arqueològica, Barcelona, Spain

*Corresponding author: Catalina Mas Florit, cmas@ub.edu
**Senior author: Miguel Ángel Cau Ontiveros, macau@ub.edu

ABSTRACT

Rural basilicas are the most important evidence of Christianization of the countryside on the island of Mallorca (Balearic Islands, Spain). Recent investigations of rural landscape transformations suggest that some churches were built along communication routes and linked to pre-existing settlements. To obtain new data that could support this hypothesis, a geophysical survey has been carried out at the early Christian complex of Son Peretó, one of the most emblematic sites for the understanding of Late Antiquity on the island. The objective was to better define the site that is undergoing excavation, and to investigate the possible presence of other constructions further than the Christian complex. The geophysical survey was carried out combining magnetometry and ground-penetrating radar. For the magnetic investigation of large site areas, a 7-probe fluxgate gradiometer array LEA MAX was used. GPR was used to examine the areas nearby the remains already excavated and to better define areas where magnetometry revealed interesting anomalies. GPR was developed by means of the IDS GPR system, which was based on the Fast-Wave module. The results revealed both the presence of architectural remains beneath the soil that help define the early Christian complex, as well as other remains that suggest the church was part of a larger settlement.

KEY WORDS: *church, Christianity, landscape, geophysics, magnetometry, GPR*

Geophysical Survey at the early Christian complex of Son Peretó (Mallorca, Balearic Islands, Spain)

Catalina Mas Florit[1,*], Miguel Ángel Cau Ontiveros[1,2,3,+], Cornelius Meyer[4], Roger Sala[5], Helena Ortiz[5], Pedro Rodríguez Simón[5]

1. Equip de Recerca Arqueològica i Arqueomètrica de la Universitat de Barcelona (ERAAUB), Spain
2. ICREA, Pg. Lluís Companys 23, 08010 Barcelona, Spain
3. Chercheur associé, Aix-Marseille Univ, CNRS, Centre Camille Jullian, Aix-en-Provence, France
4. cmp Cornelius Meyer Prospection, Berlin, Germany
5. SOT Prospecció arqueologica

* Corresponding author: Catalina Mas Florit, cmas@ub.edu
+ Senior author: Miguel Ángel Cau Ontiveros, macau@ub.edu

1. Introduction

Late Antiquity is traditionally considered to be one of the least known historical time periods of the Balearic Islands. The contribution of Christian archaeology and the investigation of rural basilicas, coupled with several survey projects on the islands (Cau 2009, Cau *et al*. 2015), have provided the first insights into the countryside during this long period (4th to 10th century AD). The Balearics changed from being an independent province within the Western Roman Empire at the end of the 4th century AD to existing under Vandal control in AD 455, Byzantine domination in AD 534, and finally Muslim rule at the beginning of the 10th century AD (Amengual 1991-1992).

Christian rural basilicas were one of the key elements of the late antique Balearic landscape, contributing to the evangelization of rural areas and playing an important role in the spatial, socio-economic, political, and religious structuring of the territory. Thus far, four basilicas have been excavated in Mallorca: Cas Frares (Santa María del Camí), Son Peretó (Manacor), Sa Carrotja (Porto Cristo, Manacor), and Son Fadrinet (Campos) (for a synthesis of the Balearic churches see: Godoy 1995; Alcaide 2011). Most of these sites are only partially excavated, focusing mainly on the architecture and liturgical organization of the religious buildings. There has been less interest in exploring the relationship between these buildings and their surrounding landscapes, although some studies have provided insight into the possible organization of the countryside and the role played by the basilicas (Mas Florit, 2013).

The study of churches is essential to understanding the shaping of Christian landscapes and the Christianization process. Many of these churches were built along communication routes both terrestrial and maritime in nature, or in nodal points on the landscape. As seen throughout the Mediterranean, the basilicas were built in preexisting and populated settlements to ensure their success. In the Balearics, there is no data to indicate whether these island churches were civil or religious initiatives. One of the main problems is the dating of the churches. In most cases, the chronology is not precise due to these buildings having been discovered and excavated at the end of the 19th and beginning of the 20th century. However, more recent excavations show that the foundation of Son Fadrinet dates from around the mid-6th century

(Ulbert 2003), and that Son Peretó was well established by the 6th century. Several surveys suggest that at the end of the 5th or in the early 6th century AD, population changes occurred throughout the countryside. The construction of the rural churches could be linked to that process (Mas Florit and Cau 2013).

Some of these churches could be placed in "secondary agglomerations" (Mas Florit and Cau, 2013); this term is used because of the inability to precisely classify the different forms and functions in which agglomerated settlements could have had within the landscape (*vicus*, *castellum*, *mansio*,...) (Bertoncello 2002; Fernández Ochoa et al. 2014; Isla 2001; Martínez Melon 2006). Although the information available on secondary agglomerations is extremely scarce, some of these rural basilicas could have been erected in these types of settlements across the countryside. In order to further investigate this possibility, the research agenda has recently introduced geophysical surveys on the rural basilicas. The main aims are to locate new constructions, assess the true extension of these rural sites, and determine whether some of these churches were built in previously inhabited settlements or secondary agglomerations.

Within the broader study of Late Antiquity settlement patterns —including geophysical prospection on rural sites—, some basilicas have been prospected. A geophysical survey of the Es Cap des Port basilica, located in Fornells Bay on the neighboring island of Menorca, showed the possible existence of ceramic kilns and other anomalies. However, no obvious traces of another large construction were found, which could support the hypothesis that this was a monastic complex (Murrieta et al., 2012). More recent yet unpublished investigations of the Son Fadrinet basilica at Campos (Mallorca) show a further complexity of the site with some additional structures apart from those already excavated.

The early Christian complex of Son Peretó in the Eastern part of Mallorca could be an example of religious building in an area of pre-existing inhabitation. In order to evaluate this hypothesis, an investigation concept was developed for the larger surroundings of the basilica. The concept consisted of a combination of field walk surveys, magnetic mapping of all relevant and accessible areas, and detailed investigations by high-resolution GPR. This approach had already proved successful in the investigation of other sites on the Balearic Islands (Mas Florit et al., 2017). In this paper we present the results of the geophysical survey, combining magnetic and GPR measurements.

2. Son Peretó: an early Christian complex

The site of Son Peretó (Manacor) is located about 6.5 km northeast of the city of Manacor in eastern Mallorca (Figure 1). Discovered in 1912, it is one of the most remarkable examples of an early Christian complex and is essential to understanding Late Antiquity in Mallorca. The site has been the subject of archaeological excavations since the beginning of the 20th century (Aguiló 1923). Excavations uncovered a church with three naves, the baptistery and an associated necropolis (Palol 1967; Palol et al. 1967) (Figure 1). Since 2005, within the framework of a new project of re-excavation, restoration, and public display of the site, several new stratigraphical sequences have aided in interpreting the site's evolution. The precise date of the church's foundation is still unknown, but it is possible that it could date to the 5th century or early 6th century. By the 6th century, the church was consolidated with a baptistery in place, which was later re-structured in the 7th century when the large font from the first phase was replaced by a smaller baptismal font (Cau *et al*. 2012; Miriello *et al*. 2013). The entire area was a necropolis with graves linked to the church, the baptistery and adjacent areas. It is also possible that the necropolis pre-dates the religious buildings. A series of domestic spaces developed during the 7th century were found located in the West Sector, attached to the baptistery. The image created is that of a small village that grew attached to the religious buildings. The entire area was destroyed by a fire at the beginning of the 8th century AD (Cau *et al*. 2012).

It is worth noting, for the purpose of this paper, that there are signs of a large necropolis in the area. At the beginning of the 20th century, casual finds showed the existence of a large variety of graves, including early imperial inhumations as well as typologies that could be dated from the 3rd century to Late Antiquity. In the church and the annexed buildings there are large quantities of inhumation graves. These graves show a variety of typologies but consist primarily in graves excavated in the soil and covered with flagstones. These would be covered by opus signinum or occasionally with mosaics, as the example of the *lauda* of Balearia indicates. The magnitude of the necropolis coupled with the presence of the baptistery and other architectural aspects (such as the capacity of the church, the largest known in the Balearics so far), may indicate that this was an important religious centre. Field walk surveys of the area in the 1980s helped to locate minor settlements not far from the basilica, which provide evidence of occupation during the Roman and the late antique periods (Mas Florit, 2006). All this information suggests that the Christian complex of Son Peretó was built on a preexisting important nucleus that corresponded to some form of rural settlement.

3. Areas of investigation and Methods

3.1. Areas of investigation

The geophysical survey was carried out using a combination of magnetic and GPR measurements. A larger extension of the fields was investigated by means of magnetic prospection. These fields surround the already excavated remains of the site enclosed by a metallic fence. A small portion of the field inside the fence was also explored with magnetometry. The magnetic measurements were executed on larger areas in the open fields to the north, northwest, northeast, southwest and west of the basilica. Additionally, a minor area inside the fenced zone to the north of the basilica was investigated (Figure 2). The terrain to the north and to the west of the basilica is even, and further to the west and the east it continues in gentle slopes. The fields' surface is characterized by grassland and harvested crops, with a few trees and bushes resulting in minor data gaps. The main sources of disturbance to the magnetic data were the wire fences around the archaeological protection zone, some power poles and the crash barriers of the Ma-15 highway passing the site. Since the measurements were carried out in the summer season, the weather during the fieldwork was hot and dry.

In a second step, GPR measurements were carried out to examine selected areas of interest in detail according to the magnetic data. Furthermore, GPR was used to explore other areas close to visible archaeological remains enclosed in the metallic fence, therefore rendering more difficult a magnetic survey. GPR survey also covered accessible areas inside the fence surrounding the excavated remains of the early Christian complex. The objective of these measurements was to detect possible building remains nearby that could be connected to the main complex. The archaeological record additionally includes features such as graves or pits excavated in the bedrock. The GPR parameters were modified reducing the time window (depth of investigation) to obtain a better vertical resolution in the shallow stratigraphical context of the site. GPR measurements were carried out inside the basilica of Son Peretó. The objective was to evaluate the contents of the subsoil, with the aim of locating the known features (mainly individual burials) and evaluating possible deeper elements not described during the excavation.

The slightly undulating landscape around the basilica offered predominantly favorable conditions for geophysical investigations of large areas. The area is intensively used for agriculture, which led to the expectation of a strong mixing of the uppermost soil layers. The geological base is formed by the Son Verdera Limestone Formation. It is composed of Middle Miocene limestones and fine-grained siliciclastic rocks with variable amounts of organic matter (Ramos-Guerrero et al., 2000). The soils that have developed as a weathering product of these rocks are predominantly silty to clayey.

A total surface of 7.75 ha was covered with magnetometry, while GPR was used in selected areas up to 2 ha. The nomenclature of the areas for the survey grids can be observed in Figure 2.

The GPR measurements focused on different areas of the site (Figure 2). The first group of dataset corresponds to the known fenced site. The prospection aimed to recognize the projection of known structures through the subsoil and to explore the immediate surroundings of the Basilica, considered the nucleus of the settlement. This survey region included three separate data acquisitions: Grid 0, Grid G2 and Grid G3. Grid 9 covered a field outside the fence, aiming to describe possible remains in the nearer limits of the known site. The surveys in this first region covered a total extension of 5052 m².

Second and third survey regions were carried out in cultivation fields at the south-west of the Basilica in order to offer additional information on the hypothesized building areas documented by the previous magnetic results. The second region covered an area of 7765 m² in three new acquisitions, called Grid 5, Grid G1 and Grid 8.

The third region, placed nearly 200 m south from the basilica, covered three different areas in active cultivation fields. These areas were called G7, G4 and G6, measuring a total area of 8174 m².

3.2. Methods

Magnetic prospection

For the magnetic investigation, an array of seven Förster fluxgate gradiometer probes mounted on a light and foldable cart was used. This gradiometer array is a component of the convertible LEA MAX system (Zöllner et al, 2011).

The Förster FEREX CON650 fluxgate gradiometer probes register the vertical gradient of the vertical component of the Earth's magnetic field with an accuracy of 0.1 nT. The measured gradient (the difference between two vertically arranged sensors in a gradiometer probe) is insensitive to the typical large fluctuations of the Earth's magnetic field and is determined only by the magnetization of local anomalies in the ground (Schmidt, 2009). The sensor separation and thus the profile distance was 0.5 m. The measurements were carried out on all accessible fields of interest surrounding the basilica of Son Peretó. The total area covered is about 7.75 hectares.

The data positioning for the magnetic survey was realized by means of differential GPS, using two GNSS receivers NovAtel SMART V1 in RTK mode (Real-Time Kinematic) to achieve a relative accuracy of 2 cm. The coordinate system in use during the magnetic measurements was WGS84 / UTM 31 North (EPSG: 32631). The coordinates of fixed points, located in the surroundings of the excavations of the basilica de Son Peretó, were used to correct the position of the base, resulting in the absolute accuracy of the positioning reaching a level of ±2 cm. After data acquisition and processing, the results were re-projected into the project coordinate system ETRS89 /UTM zone 31North (EPSG: 25831) by means of the open-source Cartographic Projections library GDAL.

After data registration, the binary magnetic data was decoded and merged with the GPS data using a script-based decoding routine (ealdec). The actual data processing was comprised of an offset and a drift correction of each channel’s data sets. Applying another script in a UNIX shell (ealmat), spike values were excluded from the correction. The maximum order of polygon fitting was set to the value of 2. All decoded and corrected profiles were subsequently summed up into one single file. This file was subjected to a gridding routine, producing a Surfer7-compatible grid with an equidistant mesh of 0.25 m. This grid file was then used to generate a GeoTIFF image that can be projected in a GIS project and served as base for the archaeological interpretation.

Interpretation base for the magnetic data

The magnetic data was interpreted qualitatively as the survey was strictly non-invasive, meaning that neither test excavations nor material sampling for laboratory testing was done. Thus, the interpretation drawings display the result of an approach that combines the knowledge of soil magnetic properties with the descriptive and comparative methods of archaeological interpretation (Neubauer and Eder-Hinterleitner; 1997, Meyer, 2013). Needless to say, the precarious character of any qualitative and comparative interpretation has to be taken into account since the reading of magnetic results can be subject to new or evolving hypotheses and knowledge.

The general approach to classifying the magnetic anomalies is to distinguish them by means of amplitude, polarization and shape. Secondly, the spatial distribution, geometric patterns and spatial interrelationships of anomalies and anomaly clusters were taken into account in the interpretation. Of course, comparative observations of similar archaeological sites and their magnetic data were of crucial importance to checking the archaeological plausibility of the interpretation (Mas Florit et al., 2018).

As part of the first step, anomalies of unambiguously modern origin —indicating ferromagnetic objects— were separated and marked. Magnetic anomalies of modern ferromagnetic objects usually show high amplitudes of the Z component of the vertical gradient. Depending on size, distance from the sensor and magnetization, they can reach several hundred Nanotesla. Moreover, these anomalies mostly have a clear dipole character. Wire fences and crash barriers along the field borders especially cause anomaly patterns of strong amplitudes and alternating polarization. Additionally, linear anomalies with both positive and negative polarization that could be associated with traces of agricultural processing such as ploughing were identified by comparison with field observations.

The second step was to sort the remaining anomalies that were assumed to have an archaeological or geomorphological background. In order to structure these anomalies, several classes were introduced with corresponding causal physical structures.

It is assumed that the local limestone of the Son Verdera Formation has diamagnetic properties. Since the predominant construction material is of local origin, linear anomaly patterns with negative amplitudes are supposed to be related to foundations and other construction remains. However, it is also expected that the actual limestone with its accompanying minerals shows a superposition of diamagnetic, paramagnetic and ferromagnetic effects, resulting in diffuse anomaly patterns with very weak negative amplitudes. This may explain the difficulty of identifying ancient construction remains in the magnetic data, and also provides justification for using the GPR as a complementary method.

Besides the limestone constructions, other archaeological features can be identified in the magnetic data. Firstly, circular and rectangular positive anomalies with low amplitudes and extensions between 1 and 4 meters are attributed to pit fillings. These structures can reflect construction pits in relation to the building remains, working and storage pits, and burials in the surroundings of the basilica. An archaeological interpretation of these types of anomalies is only possible with consideration of their spatial context. The weak positive values of the magnetic gradient originate in an increased magnetization, where both induced and remanent magnetization occur. The induced magnetization is caused by an increased content of ferrimagnetic iron oxides in the pit fillings, which is in turn caused by the conversion of low magnetized iron oxides into ferrimagnetic oxides (such as maghaemite and magnetite in combustion processes) and by microbiotic influence (Fassbinder, 2017). Secondly, anomaly patterns showing similar amplitude and polarization characteristics with a linear geometry are associated with ditch fillings.

Furthermore, numerous magnetic dipole anomalies with medium amplitudes and north-south orientation of the dipole were observed. Since these anomalies occur in clusters and are found inside the assumed ancient buildings and their surroundings, they were considered accumulations of predominantly thermoremanent material, indicating remains of furnaces, hearths or other human-made fireplaces. Features of this type were observed and described at numerous Roman and other archaeological sites (Neubauer and Eder-Hinterleitner, 1997; Linford and Canti, 2001).

Eventually, magnetic anomalies reflecting natural structures and features were identified. Elongated or extensive zones with apparent irregular order of strong positive and dipole anomalies were compared with terrain steps and bedrock outcrops at the surface. In several cases a spatial correlation was found, so these zones can be connected with the outcropping bedrock. The cause of the complex anomaly patterns remains unclear. It is assumed that the high amplitudes of the magnetic anomalies are related to magnetized material found in veins of the weathered limestone.

A second class of natural effects are magnetic anomalies coming from lightning strikes. Amplitude and polarization are often similar to magnetic anomalies from remains of ovens, however they lack context within an archaeological site and are found at highly exposed sites. Depending on the geological conditions, these anomalies have a dipole or multi-pole character and very variable shapes, including long curved lines or butterfly shapes (Jones and Maki, 2005).

All anomaly classes described are presented in different shades of grey and hatchings in the interpretation drawings (see legends). For reasons of clarity, the anomalies of modern origin are not displayed on the interpretation maps.

Ground-Penetrating Radar (GPR)

The areas were surveyed using an IDS GPR custom system based on the Fast-Wave module that collects data simultaneously from five 600 MHz antennas, placed parallel on a survey cart. The spatial resolution was established on 0.2 m between profiles, at an in-line resolution of 27 scans per meter. The time-window was fixed on 60 nanoseconds, resulting in an effective depth range that varied from 1,2 m to 1,5 m, at an estimated velocity of 0,1 m per nanosecond. This approximate velocity range has been estimated by measuring hyperbola shapes on single profiles.

The GPR data was collected using local coordinates and orthogonal grids adapted to the geometry of each survey site. Afterwards, control points were taken by a GPS Leica GG02/Zeno 5 to re-project the grids to absolute coordinates.

The data processing was made using GPR-Slice software to produce sequences of time-slices at increasing depths as well as vectorial maps of reflective anomalies. These views are used as the base outputs to create the final interpretation diagrams in the GIS project.

The data treatment consisted of two phases: correction of 2D profiles and generation of time-slice sequences. Raw data profiles have been processed by applying a band-pass filter to correct the phase-drift and low-frequency noises, and a gain function to compensate for amplitude decay with depth. A further background removal was applied to correct constant noises produced by the system and to enhance the detection of short-scale anomalies (Conyers and Goodman, 1997).

The time-slice sequences were produced by resampling the processed 2D profiles in 16 slices of 3,75 nanoseconds, representing an estimate lapse of 0,19 m each, in a total depth range from 0 m to 1,52 m. The overlap thickness between slices was set at 50%. The resulting plots have been resampled to a resolution of 0.1 m x 0.1 m, and finally filtered using a Gaussian low-pass filter of 3X3 cells (30 cm). The resulting maps were imported to the GIS project, where further interpretation steps have been done. The vectorial maps of reflective anomalies by depth were generated using the depth-threshold function by GPR-slice software. The function consists in alternative, binary output plots of time-slice sequences, which include only anomalies up to a given amplitude value (Goodman and Piro, 2013; Schmidt and Tsetskhladze, 2013). These plots are converted to vectorial polygons using Qgis software and merged in a single shape file. The resulting maps were expressed as a classed diagram by assigning a range from light to dark colors to anomalies detected from shallow to deep features.

Since the data quality and contrast varied substantially in the different acquisitions of the GPR surveys, the threshold values used to create the vectorial maps of anomalies were established using a general value of 1.5 standard deviation plus/minus the mean of each time-slice. Afterwards they were corrected manually, especially in the case of grids that include high reflective bedrock outcrops (Grids 5, 6, 8 or 9).

Data quality and interpretation parameters for GPR

The original GPR data showed quality flaws because of two main factors. Firstly, the local geology formed by clayey soils and limestone offered a good contrast between sediments and bedrock, but a limited penetration even in very dry conditions (Verdonck, 2012). However, all data was collected at high temperatures and dry conditions, which probably limited the detection of subtler stratigraphical features yet produced high-contrast anomalies for building structures made by local stone. The second factor that conditioned the data quality is the ground contact of the antennae in Grids G1, G2 and 5, where the resulting data sets show frequent anomalies produced by miscontacts and a poorer geometrical definition of building remains in the final time-slice views. Taking into account these factors, the interpretation of the GPR results summarized in the synthetic interpretation diagrams include five categories: bedrock, debris/ heterogeneous fillings, building features, not identified and burials. Some of these cases are illustrated in Figure 3, showing a time-slice of the southern region of the site and radargrams crossing a debris layer (radargram D), a group of walls (radargram E), and a limestone outcrop (radargram F), as well as an example of single profiles over a burial that will be illustrated in the GPR results section.

4. Results and discussion

4.1. Magnetic prospection and its results

The results of the magnetic survey are displayed on a map as greyscale images with dynamics of ±6nT (Figure 4), and the interpretation can be found on Figure 5.

The immediate surroundings of the basilica were not surveyed due to the presence of excavation trenches and wire fences. Inside the fence and to the northeast of the church's remains, an area of only 3,000 m^2 could be investigated. Trees and bushes caused several gaps in the data set. The results show a considerably higher contamination of modern elements and only a few indications of construction remains in the ground. Negative linear anomalies suggesting the existence of foundations made of local limestone are only visible in the western part of the area, close to the basilica. The eastern part is characterized by positive oval to circular anomalies, indicating fillings of pits. One structure —a distinct dipole anomaly of moderate amplitudes located at the northern edge of the area— may be connected to the remains of an oven or hearth.

The results obtained from the field southwest of the basilica distinguish features unequivocally related to archaeological remains. A set of negative linear anomalies in the data has been interpreted as a complex of walls; the foundations seem to form the remains of a rectangular building almost perfectly matching the orientation of the basilica. Around and inside the presumed buildings, irregularly shaped positive anomalies indicate ditches or fillings. In addition, circular positive anomalies indicating pits occur in and around the buildings. Both groups of anomalies may also point to the remains of burials.

Further southwest, negative linear anomalies of circular or rectangular shape indicate the remains of other building structures. These anomalies are again associated with positive anomalies indicating pits and ditches. Some circular anomalies are likely to be associated with economic activities of some kind, possibly reflecting reused deposits. In addition, positive oval-shaped anomalies with an average length of 2 m occur in concentrations around the building structures and are linked to burial activity. Further to the southwest, at a distance of 150 to 200 m from the basilica, the magnetic anomalies caused by foundations of buildings fade out. The character of the magnetic anomalies changes to groups of circular anomalies, both positive and dipole, originating in pit fillings and remains of hearths or ovens. These structures are scattered over an area of approximately 3,400 m^2, possibly revealing an ancient production area.

The most conspicuous structures formed by the magnetic anomalies are found even further southwest, at a distance of more than 200 m from the basilica. At the northern edge of this area, a regular pattern of strong dipole anomalies covering an almost rectangular area of 150 m^2 suggests the existence of a great volume of burnt, i.e. thermoremanently magnetized, material. In its surroundings, further rectangular positive anomalies and linear negative anomalies are unmistakable signs of the existence of a larger ancient building complex with dimensions of at least 50 m by 35 m. In order to prove this assumption and obtain more detailed information, GPR measurements were carried out in this zone (see below). The strong thermoremanent anomalies and their regular shape can be explained by the existence of remains of a large oven complex, probably used to supply a hypocaust heating.

These structures related to this large building complex possibly continue to the west. Indications of foundations and walls can be found in the data up to a distance of 175 m to the west of the basilica. At the northern limit of the surveyed area, some circular magnetic anomalies indicate the existence of burnt material originating from remains of ovens, kilns, or other fireplaces in the ground. Since the building structures in the west lack of clarity, it can be assumed that the degree of preservation decreases from the center to the western margins. Furthermore, magnetic data shows that this building complex continues to the north. Negative magnetic anomalies suggest the existence of a rectangular building, closing the main building to the north. Inside the foundations, some circular and oval anomalies of higher amplitudes point to remains of combustion from ovens, kilns, or hearths.

The area west of the agglomeration of buildings and north of the large building complex is largely free of clear structures. Outcropping bedrock can be traced at the western end and in the center of the surveyed area. Some linear structures may refer to water pipelines or enclosure walls of unknown dates. In the centre of this apparently empty area, a high-amplitude magnetic anomaly of butterfly shape likely shows the thermoremanent effect of a lightning strike.

The results of the measurements to the north of the basilica show areas with dense clusters of mainly positive magnetic anomalies. However, they cannot be connected with ancient building structures. These large and irregular patterns can also reflect quarries used for the extraction of building material. The center of the northern area is still occupied by the ruins of a farmstead, presumably of the 19th or 20th century. The high concentration of circular positive magnetic anomalies located around these ruins can be related either to this farmstead or to an earlier construction phase. To the north-northwest of the basilica, the results of the magnetic data do not allow for a satisfactory interpretation. In contrast to the area in the southwest, archaeological remains are less distinguishable with only a few positive anomalies reflecting pits and ditches. The data obtained from the area further to the basilica's northeast gives no insight into the archaeological situation due to dominant modern disturbances and assumed absence of archaeological features, possibly due to their destruction in recent times.

4.2. GPR measurements and its interpretation

The basilica and its surroundings

The magnetic survey coverage was partial, as the presence of several metal displays and the metallic perimeter fence produced a magnetic disturbance on the signal. Thus, the

GPR datasets obtained in this region lack the support of other geophysical data to refine the interpretation of GPR results.

The excavations revealed a group of buildings disposed according to the orientation of the basilica as the nucleus of the settlement. The stratigraphic record has shown a variable vertical dimension in the whole area, as bedrock outcrops and even structures cut in the bedrock have been documented. The GPR data obtained in this area shows a response consistent with this subsoil disposition, detecting highly reflective and extensive anomalies identified as limestone bedrock outcrops that alternate with slightly less reflective features identified as building remains.

Grid G3 covered the area inside the basilica (Figure 6), showing buried graves and pavements. It also showed the bedrock horizons in the southeastern corner and in the center of the explored area (Groups 72 and 76). Vectorial maps by depth show how groups of burials are clearly detected (Groups 78, 79, 80, 81 and 82), as well as pavement remains near the southeastern apse (75). In the same depth range and in the northwest corner of the basilica, another group of burials (84) was detected. Below those burial levels, several features were identified but with no clear correlation to excavation information. In the northern corner of the grid, Group 73 shows high reflection amplitudes, probably indicating an altered bedrock rise. Parallel to the southern wall of the basilica, two anomaly groups (77 and 83) show high reflection amplitudes at depths of more than 0,6 m (GPR profiles in Figure 6). Although the shape of anomalies change with depth, their high amplitudes indicate that they may be a product of heterogeneous fillings or even building remains. Similarly, the anomaly Group 72 increases in extension with depth.

Grids 0 and G2 covered the accessible areas around the excavated remains of the settlement (Figure 7). The resulting time-slice sequence from Grid 0 offered a similar quality as the data obtained inside the basilica building. A topographical slight descending slope to the south-west and multiple local changes in elevation produced both by the excavations and the previous cultivation works resulted in the depth of detected features not showing a regular trend in the two grids (where shallow bedrock outcrops and building remains could be found at variable depths).

Two main groups of linear anomalies are described to the west and north of the known remains. The Groups 15, 16, 17, 18 and 19 are identified as possible wall remains. Although the detection of these features looks consistent in the time-slice sequence, only Groups 15, 18 and 19 seem to match with the geometry of surrounding excavated buildings. Groups 16, 17 or 21 show no evident connection to other structures.

In connection with Group 15, an extensive anomaly called Group 14 is interpreted as a bedrock rise. It also contains internal variations that have been interpreted as a group of three independent burials (Group 13).

To the north of the main building complex, the results show a region where no clear features are identified. Groups of reflective anomalies with no clear geometrical definition such as 25, 26, 27, 28, 29, 30 or 31 are alternatively interpreted as regions of heterogeneous fillings or non-identified structures. To the north of this fringe with no clear structures, the Groups 32 and 35 were detected and identified as two burial concentrations.

Although trees and bushes in the survey area did not allow a total coverage of the northern limits of known buildings, the data points to a new region at the north of the basilica containing building remains and unidentified features.

The anomaly Groups 36, 40, 41 and 43, detected between depths of 0,3 m to 0,8 m, have been identified as possible walls, apparently following the orientation of the basilica. But, other linear features detected in the same zone as 37 and 39 show no clear connection with other structures. At the north of the basilica, the anomaly Groups as 42 and 38 are interpreted as new groups of graves.

The Grid 0 also included a part of the path that runs by the south-west with the site fence. Here, two highly reflective anomalies called 23 and 24 have been identified as possible remains of the path's gravel pavement. Group 22, composed of three weaker linear anomalies, has been interpreted as part of a new building structure and maintains a similar orientation of closer excavated buildings.

The northern area of the site enclosure was explored in a new data acquisition called Grid G2. This region was partially cleared from vegetation a few days before the survey, leaving an uneven surface with frequent stumps and shallow roots. Consequently, the datasets obtained from the GPR survey show a poorer quality than Grids 0 and G3, mostly because of the irregular contact of antennae with the ground. The vectorial map of anomalies by depth (Figure 7) shows a spread of small reflective features produced by the transitory contact faults of the antenna stack, and only few anomalies have been considered as possible archaeological remains or old cultivation tracks. Groups as 55, 56 or 52 have been identified as possible building features due to their apparent linear shapes, but their poor definition in the time-slices in a noisy context introduced doubts regarding that attribution. In a similar context, the anomaly Groups 46, 47, 48, 50, 51 and 52 have also been interpreted as possible walls or agricultural structures of short vertical dimension.

Grid 9 partially covered up an almond-tree field placed at the south-east of the basilica, outside the fenced site (Figure 8). The resulting time-slice sequence shows three high reflective areas from 0,25 m depth, labeled as 121, 110 and 111. These regions are interpreted as limestone basement. However, some internal variations in the response suggest possible structures cut in the bedrock or connected to it. Groups 120 and 122 have been identified as possible archaeological features at up to 0,7m depth, although the poor definition of their geometries and the lack of other information on the area resulted in their consideration as nonconclusive.

A similar case was described for the anomaly Groups 110 and 111. They consist in two fringes giving a reflective response, crossing the field from north-east to south-west. The time-slice sequence demonstrates that these reflections are not parallel to the surface, showing a descending slope to the north-east. According to these characteristics, both groups have been interpreted as new bedrock outcrops. But again, a number of weak reflection anomalies in its surroundings or connected to them (Groups 112, 113, 114, 117) suggest that the bedrock outcrops could have been used as a base for anthropogenic structures, as limits of cultivation terraces, or other building structures.

In the central region of the Grid 9, some other weak anomalies were detected. However, they offer no clear evidences of a consistent group of buildings. Alterations like 115, 116, 119 or 124 show subtle changes in reflection and short vertical projections, but evident linear trajectories. These factors suggest they could correspond to agricultural structures. Only Group 118 has been identified as a possible building remain, containing some possible walls and a reflective area identified as a deposit of heterogeneous fillings.

The second region explored using GPR covered the survey Grids G1, 5 and 8 at the south of the path leading the site. In this case, the objective of the GPR measurements was to broaden the information brought by the previous magnetic surveys in selected parts of these fields. As it has been exposed in the previous section, the magnetic maps of this region show a highly disturbed magnetic response where multiple focus anomalies and linear features of negative magnetic values are visible.

The Grids G1 (1573 m²) and 5 (2563 m²) were placed in order to cover the main concentration of magnetic anomalies interpreted as being related to archaeological features. Grid 8 (1640 m²) at north-west of Grid 1 aimed to offer alternative data on an area where subtle linear features have been detected in the magnetic survey.

In Grids G1 and 5, the rugged surface produced a noisy dataset, but the time-slice sequence allows the recognition of new zones of archaeological interest. A minimum of two building groups have been identified in the area of Grid G1, and a new group of possible burials appears in the north corner of Grid 5. In the southern half of Grid 5, a new bedrock rise produced a very complex response.

As shown in Figure 9, these building remains can be easily identified below the cultivation layers. The main anomaly groups can be defined at a depth of 0,4 m, but time-slices of deeper layers show that the features located in the north disappear (Groups 69, 70 and 71) and indicate poorer conservation. In the western corner of the grid, a fringe showing high reflection amplitudes can be explained by the existence of a shallow bedrock layer.

The anomaly Groups 63 and 108 are considered to be the main parts of buildings, defining a possible patio or open space in between structures (Group 109). A third feature called Group 64 seems to constitute another building clearly connected with the main Groups 63 and 108, despite showing a different orientation and possibly indicating a different construction phase.

To the west of these buildings, a group of diffuse and reflective anomalies show areas interpreted as debris deposits or other not determinable building remains. The southern and eastern perimeters of the building Group 108 show other linear features (Groups 62, 65, 66) which can also be ascribed to building remains or partially conserved rooms.

The anomaly Groups 69 and 70 show new linear alterations interpreted as building remains. The time-slices between the depths of 0.25 and 0.7 m allow for the recognition of a rectangular room measuring nearly 9 m x 4 m and following an east-west orientation. Although the western part of the room seems to be destroyed, the eastern limit is clearly visible in addition to other less defined features to the south (Group 69).

The Group 68, located in the south of Grid 1, shows an area containing diffuse and reflective anomalies, interpreted as heterogeneous fillings or a debris layer. In this case, the depth of these structures suggest that the assumed building remains were partially destroyed by agriculture activity.

By chance, a cavity was discovered during the survey works. The data obtained above this cavity shows a weak contrast, but the hyperbola produced by the cavity is clearly visible in the profile raw data. A similar response was detected 9 m to the southeast of this location, possibly revealing another cavity (Figure 10). The origin of this feature is uncertain.

In Grid 5, reflective features appear to be concentrated in the southern half of the grid from 0.1 m to 0.4 m depth. The images obtained from these features are interpreted as a heterogeneous layer in contact with bedrock outcrops, also containing debris levels and some subtle linear features which are interpreted as possible building remains.

Anomaly Groups 129, 130, and 134 are larger areas of high reflection amplitudes. However, these reflective areas show a spread of some weak linear anomalies which could be remains of walls or cuts in the bedrock. Anomaly Groups 131 and 132 show similar responses until depths of 0.70 m to 0.90 m.

Group 125 designates a new area in the center of the grid where almost no reflective features were identified, except for a subtle linear limit at its north (Group 126). According to this response, Group 125 has no conclusive interpretation as it could correspond to a lower bedrock area filled with regular sediments or be representative of other anthropogenic features.

The anomaly Group 127 shows similar characteristics as defined for the southern groups (131, 132). Indeed, a number of weak linear and extensive features are detected, but the images and data are not conclusive enough to relate them to building remains.

In the northeast corner of the grid, a new group of features (123) is detected from 0.6 m depth. It consists of a sum of reflective linear features pointing southeast. According to the characteristics of the response, similar to other burial groups described around the Basilica, the Group 123 is interpreted as a burial area containing at least 10 burials.

In Grid 8, a new shallow outcrop of bedrock occupies the north-east half of the explored area, producing a highly reflective response from 0.35 m depth (Group 139). In the shallower slices, some local and weaker features such as Group 140 suggest possible building remains or cuts in the bedrock, but a relation of these features to the actual building a few meters to the north cannot be discarded.

The most remarkable groups are 143 and 144 as they show a linear geometry and a response compatible with wall remains. Although their reflectivity values are weaker, Groups 145, 142 and 146 could also be interpreted as building remains.

A third region was explored nearly 200 m to the south-west of the basilica, where the magnetic maps revealed two concentrations of strong magnetic anomalies interpreted as a possible group of building features. These areas were explored with GPR in three new survey areas: Grid G4 (3170 m²), Grid 6 (3773 m²), and Grid 7 (1088 m²).

The time-slice sequence produced from the Grid 4 GPR survey reveals a significant group of linear and extensive anomalies, detected immediately beneath the cultivation layers that have been interpreted as remains of a main building group (Figure 11). The data shows that the shallowest features connected to the building are located at a depth of 0,25 m here. Several linear features appear surrounded by diffuse and highly reflective structures, presumably debris accumulations and heterogeneous fillings caused by plough works.

At a depth range of 0.35 m to 0.45 m, the building complex appears to the full extent, revealing a structure with at least three building sections. A large section includes the anomaly Groups 86, 87, 88 and 89, forming a rectangular perimeter of 22 m x 18 m inside it. Groups 88 and 89 show almost no internal subdivisions, while Groups 86 and 87 present well defined rooms and internal walls. Group 87, which consist of two elongated rooms of approximately 12 m x 2.5 m each, is defined by high reflection amplitudes over its entire extension between 0.25 m and 0.6 m depth.

This pattern of anomalies can be explained with the occurrence of a debris layer covering those rooms. Another adjacent room (95) is detected at the southwestern corner of this building section. Further to the south, an open area probably defines some sort of a patio, limited at the east by a clearly visible wall (85).

A second building section is defined by the anomaly Groups 90, 91, 93, 94, 95, 96 and 97. Despite an orientation of some of the walls consistent with the structures of the first section, the rooms show a poorer definition. This was interpreted as a product of massive debris accumulations and is especially visible in the Groups 93 and 94. A slight change of orientation can be observed in the area of the Groups 91 and 92, probably indicating different construction phases.

A third structure with a ground plan of 23 m x 12 m is interpreted from the anomaly Groups 102, 103, 104 and 105. In this particular case, the internal divisions of the building can only be roughly estimated, probably because of debris layers.

In the eastern part of the grid, some irregularly shaped anomaly groups may also be ascribed to buried building remains (98 and 101) in poorer preserved conditions than the ones in the western part. To the east, the anomaly Groups 99 and 100 possibly correspond to bedrock rising up to depths of approximately 0.3 m.

The Grid 6 covered an area where high-contrast magnetic anomalies were previously detected in an extension of nearly 3000 m², at 25 m south of the main building bodies detected in Grid G4. The southern quarter of the grid is occupied from shallow depths onward by an intense anomaly group interpreted as a bedrock outcrop, where clear linear interruptions are described (150-151-152 or 157).

The most significant anomaly groups are detected from 0.4 m to 0.8 m depth, including linear features 158, 166, 160, 169 and 155. In all cases, these reflective anomalies are compatible with building remains. However, it is important to remark that this means no necessarily walls, especially if we take into account an agricultural environment. Other features as channels or filled ditches could produce a similar response.

In the center of the grid, where more intense magnetic anomalies were detected, the GPR data showed only subtle anomalies as in Groups 161, 164, 165 and 168. A possible explanation for this different response between magnetic and GPR data could be that the anomalies are produced by deeper objects or by local thermal alterations. In any case, the apparently unconnected linear features (158, 159, 160,150) could also be related to a possible production area without discarding recent agricultural features (Figure 10, 11). Other features placed in the limit of the field (162 and 163) are also interpreted as possible building remains.

Grid 7 was placed in the field contiguous to the north limit of Grid 4 to investigate possible continuity of the main building group. The results of the time-slice sequence do not show clear building features. A group of highly reflective anomalies called 171 was detected at the north of the grid from surface levels onward. The morphology and response of that anomaly group suggests a new bedrock outcrop. The area occupied by the strongest magnetic anomaly (173) shows no evidence of possible walls, indicating that the magnetic anomaly was likely produced by fillings of more magnetic sediments moved by ploughing.

4.3 Discussion

The survey strategy included the magnetic prospection as the adequate method for large-scale recognition of archaeological features within the wider surroundings of the basilica of Son Peretó, while the GPR served as a method to obtain more accurate geometrical descriptions and depth information of the localized structures. Nevertheless, the areas which were investigated with the two methods revealed the complementary of both geophysical data.

A good example is the southwestern region, where both data sets revealed the existence of a large building complex and a possible production area. Comparing the results of the magnetic survey and the GPR data, it is evident that the description of this survey region would be different if the area had been explored using just one of the two methods (Figure 12). The presence of building remains, suggested by the magnetic data, was also confirmed by the GPR data on Grid G1.

On Grid 6, the southern GPR acquisition revealed almost no evidence of structures, apart from some linear anomalies interpreted as possible building remains or filled channels. However, the magnetic data for the same area revealed an important concentration of magnetic anomalies indicating both the presence of thermoremanent material and pit fillings, which are probably related to kilns and pottery production.

On Grid 4, where an extensive building complex was identified, the magnetic and GPR data sets also proved to be complementary. Indeed, the most remarkable magnetic anomalies consist of elongated dipole anomalies, which perfectly match the GPR results. Not only the shape of the structures 86 and 87 are similar in both data sets, but the GPR data also suggests a debris layer on top. This could be one cause of the high magnetic values measured, assuming that the debris layer contains ceramic, i.e. thermoremanent building materials, such as *tegulae* or *opus signinum* remains.

A comparison of magnetic and GPR data further shows that the magnetic data reflects the bedrock outcrops only when they are related to vein fillings of the weathered limestone, while the GPR shows larger bedrock layers already in shallow depths, seen in Grids 5, 6, and 8. The absence of magnetic anomalies at these sites suggests that the largest part of the bedrock consists of more or less homogeneous diamagnetic limestone, and only the inhomogeneities of the weathered limestone layers (i. e. veins with highly magnetized fillings) are displayed in the magnetic data. Additionally, the measured value of the vertical gradient of the Z component is largely insensitive to magnetic field changes over large areas and at greater depth. For the magnetic investigation of the bedrock layer, a total field measurement with Caesium magnetometers would be recommended.

The geophysical survey was undertaken with a clear initial hypothesis that the basilica was not isolated but built in a nucleus of pre-existing population. The dimensions and capacity of the church, the large extension of its necropolis, the significant refurbishments completed over the course of time, and the importance of its baptisteries suggested that this Christian complex was an important religious center in the territory. The presence of the funerary inscription of *Bassus,* a priest from the Holy Roman Church, in the cemetery supports this assertion. All this evidence denotes the importance of the Christian community linked to the basilica and opened the possibility of the existence of an important settlement.

Of course, geophysics has been applied before to the study of Christian basilicas from different periods in other parts of the Mediterranean; its application helped to investigate buildings both in urban (e.g. Cozzolino et al. 2018; Tsokas et al. 2007) and rural settings (e.g. Apostolopoulos et al. 2015). In our case, although we certainly explored the basilica and its immediate surroundings, the primary object of attention was the nearby landscape as we attempted to verify whether it was an isolated construction or formed part of a wider settlement. A similar methodology was applied to the basilica of Es Cap des Port in Minorca, where, in a more limited extension, the geophysical survey was able to locate productive areas likely related to pottery production in what could be a monastic complex (Murrieta et al. 2012). In the previous and still unpublished results of the Christian basilica of Son Fadrinet in Mallorca, the existence of other constructions apart from those already excavated were also demonstrated.

In Son Peretó, the results of the geophysical investigation show some traces that are linked to the already known early Christian complex. This is the case of some anomalies corresponding to several graves that reveal the continuation of the necropolis. Some walls in other fields surrounding the excavation seem to have a similar orientation to those exhibited by the ecclesiastical complex and its annexes. Nevertheless, the presence of other remains at a relative distance and with a different orientation, as well as the quantity of poorly defined traces scattered in the surrounding fields, show a major complexity of the settlement. It is particularly important to note that the large building found in Grids G7, G4 and G6 and measuring a total area of 8174 m², could correspond to some of the forms of rural occupation (Roman *villa*, *mansio*,...) (Fernández Ochoa et al. 2014). Although it is better to be cautious with the exact identification of this building, the results confirm the hypothesis that the early Christian complex was not isolated and built in a pristine location, but instead erected in a place with a preexisting population. This is a major change in our understanding of the site and its significance. Although there is a tendency to identify rural Roman sites as *villae*, there are other forms of occupation in the countryside. The fact that Son Peretó could also be linked to a communication route —something that we have explored somewhere else (Mas Florit et al. in press)— cannot rule out the possibility of a *mansio*. The results allow us to hypothesize the presence of a *villa* or *mansio*, of Roman origin —as suggested by the surface ceramic materials— that was transformed in Late Antiquity and where the ecclesiastic complex was erected. Also, the large extension of constructions scattered throughout the area could point to the presence of a *vicus* or small village. Of course, this would have to be confirmed with archaeological excavations in order to understand the chronology of all the archaeological remains scattered through the area (they could not all be contemporary), and the exact character and typology of the constructions.

Conclusions

The geophysical survey, using a combination of magnetometry and GPR, has proven to be successful in locating archaeological remains in the area of Son Peretó. The presence of what can be interpreted as the remains of a relatively large Roman *villa* or other form of rural occupation not far from the church is a major discovery. This suggests that a Roman building evolved into some kind of secondary agglomeration that was finally Christianized with the construction of the religious complex.

The results of the geophysical survey substantiate the hypothesis that the ecclesiastical complex of Son Peretó was not isolated, but instead erected in a previous settlement. Of course, archaeological excavations are needed in order to crosscheck the information provided by geophysics, but the results so far are promising for future excavations and have contributed to a change in the site's interpretation as a whole.

Acknowledgements

This contribution forms part of the results of the project *Archaeology, Remote Sensing, and Archaeometry: A multidisciplinary approach to landscape and ceramics from the Roman to the Medieval period in Mallorca (Balearic Islands)* (ARCHREMOTELANDS) (HAR2017-83335-P), PI: Miguel Ángel Cau Ontiveros, funded by the Ministerio de Ciencia, Innovación y Universidades, with contribution from the European Regional Development Fund from the European Commission. The results are also part of the project *Remote Sensing, Geophysical Survey and Paleoenvironmental Reconstruction of the Mallorcan countryside*, financially supported by the Consell de Mallorca, PIs: Catalina Mas Florit and Miguel Ángel Cau Ontiveros. This is also part of the activities of the Equip de Recerca Arqueològica i Arqueomètrica de la Universitat de Barcelona (ERAAUB), Consolidated Group (2017 SGR 1043), thanks to the support of the Comissionat per a Universitats i Recerca del DIUE de la Generalitat de Catalunya. The work of C. Mas Florit was possible thanks to a Beatriu de Pinós postdoctoral fellowship from the AGAUR, with the support from the Secretaria d'Universitats i Recerca of the Departament d'Economia i Coneixement of the Generalitat de Catalunya, as well as to a Juan de la Cierva-Incorporación contract, funded by the Ministerio de Ciencia, Innovación y Universidades.

We are most grateful to the owners of the fields surrounding the site of Son Peretó for their permission to survey the different lands, to the City Council of Manacor, and to the current project and team of archaeological excavations for their support. We are also grateful to Peter Lanzarone, to an anonymous reviewer, and to the editors for their helpful comments that have certainly helped improve the final version of this paper.

References

Aguiló, J. 1923. Un descubrimiento arqueológico en Manacor, o un nuevo argumento de ortodoxia final de Grande Osio de Córdoba. *Boletín de la Sociedad Arqueológica Luliana* 19: 204-207; 245-248; 257-259.

Amengual, J. 1991-1992. *Els orígens del Cristianisme a les Balears i el seu desenvolupament fins a l'època musulmana*, Vol. I-II, Editorial Moll: Mallorca.

Alcaide, S. 2011. *Arquitectura cristiana balear en la antigüedad tardía (ss. V-X d.C)*, Ph.D. Dissertation, Universitat Rovira i Virgili, Tarragona, (http://www.tesisenred.net/handle/10803/32933).

Apostoulos, G., Minos-Minopoulos, D., Pavlopoulos, K. 2015. Geophysical investigation for the detection of liquefaction phenomena in an archaeological site, Lechaion, Greece. Geophysics 80 (4): EN105–EN117.

Bertoncello, F., 2002, Villa/vicus: de la forme de l'habitat aux réseaux de peuplement. *Revue archéologique de Narbonnaise* 35: 39-58.

Cau Ontiveros, M.A. 2009. Las Baleares durante la Antigüedad tardía: investigaciones recientes en un sistema insular. *Mainake* XXXI: 63-70.

Cau, M.Á., Albert, R.M., Gurt,J.M., Martínez, V., Mas Florit, C., Pecci, A., Reynolds, P., Ripoll, G., Tsantini, E., Tuset, F. 2015. Equip de Recerca Arqueològica i Arqueomètrica de la Universitat de Barcelona (ERAAUB) (1992-2015). *Pyrenae*, Número Especial 50è Aniversari: 181-244.

Cau M.A., Riera Rullan, M. and Salas, M. 2012. The early christian complex of Son Peretó (Mallorca, Balearic Islands): excavations in the 'West Sector' (2005-2008), *Archeologia Medievale* XXXIX: 213-225.

Calia, A., Leucci, G. Masini, N., Matera, L., Persico, R., Sileo, M. 2012. Integrated prospecting in the crypt of the Basilica of Saint Nicholas in Bari, Italy. *J. Geophys. Eng*. 9: 271–281

Conyers L., Goodman D. 1997. *Groud-Penetrating Radar: An Introduction For Archaeologists*, Altamira Press:Walnut Creek, CA.+

Cozzolino, M., Di Giovanni, E., Mauriello, P., Piro, S., & Zamuner, D. 2018. *Geophysical methods for cultural heritage management*. Springer.

Fassbinder, J. W. 2017. Magnetometry for archaeology. In *Encyclopedia of Geoarchaeology,* Gilbert, A (ed.). Encycl. Earth Sci. Series*,* 499-514.

Fernández Ochoa, C., Salido Domínguez, J., Zarzalejos Prieto, M. 2014. Las formas de ocupación rural en Hispania. Entre la terminología y la praxis arqueológica. Cuadernos de prehistoria y arqueología 40: 111-136.

Godoy, C. 1995. *Arqueología y liturgia. Iglesias Hispánicas (siglos IV-VIII)*. Universitat de Barcelona-Port de Tarragona: Barcelona.

Goodman, D., Piro, S. 2013. GPR Remote Sensing in Archaeology. In *Geo-technologies and the environment* (Vol. 9, XI). Berlin: Springer.

Isla, A. 2001. Villa, villula y castellum. Problemas de terminología rural en época visigoda. *Arqueología y Territorio medieval* 8: 9-19.

Jones, G., Maki, D. L. 2005. Lightning-induced magnetic anomalies on archaeological sites. *Archaeological Prospection*, *12* (3): 191-197.

Linford, N. T., Canti, M.G. 2001. Geophysical evidence for fires in antiquity: preliminary results from an experimental study. *Archaeological Prospection* 8 (4): 211-225.

Martínez Melón, J.I. 2006. El vocabulario de los asentamientos rurales (siglos I-IX d.C.): evolución de la terminología. In *Villas tardoantiguas en el Mediterráneo* *occidental*, Chavarría A., Arce J., Brogiolo G.P. (eds.). Anejos de Archivo Español de Arqueología XXXIX: Madrid; 113-31.

Mas Florit, C. 2006. *Cerámica y poblamiento durante la Antigüedad tardía (ss. IV-X) en la isla de Mallorca: la zona este (Manacor y Sant Llorenç)*, M. Phil Dissertation. University of Barcelona.

Mas Florit, C. 2013. *El poblamiento de Mallorca durante la Antigüedad tardía: la transformación del mundo rural (ca. 300-902/903 d.C)*, Ph.D. Dissertation, Universitat de Barcelona, Barcelona (http://hdl.handle.net/10803/109048).

Mas Florit, C., Cau, M.A. 2013. Christians, peasants and shepherds: the transformation of the countryside in late antique Mallorca (Balearic Islands, Spain), *Antiquité Tardive* 21: 27-42

Mas Florit, C. M., Ontiveros, M. Á. C., Goossens, L., Meyer, C., Sala, R., & Ortiz, H. 2018. Geophysical survey of two rural sites in Mallorca (Balearic Islands, Spain): unveiling Roman villae. *Journal of Applied Geophysics*, *150*, 101-117.

Meyer, C. 2013. Interpretation and Guidelines for Reporting. In *Good Practice in Archaeological Diagnostics*, Corsi, C. Slapšak, B., Vermeulen, F. (eds.). Springer, Cham, 177-190.

Mas Florit, C., Murrieta Flores, P., Wheatley, D. W. y Cau, M. A. in prenss. Communication routes and basilicas: Shaping the Christian landscape in Late Antique Mallorca (Balearic Islands). In *Las islas Baleares durante la Antigüedad tardía (siglos III-X)*, M.A. Cau (ed.). Limina-limites: archaeologies, histories, islands and borders in the Mediterranean (365-1556), Archaeopress.

Miriello, D., Bloise, A., Crisci, G. M., Cau Ontiveros, M. Á., Pecci, A., Riera Rullan, M. 2013. Compositional Analyses of Mortars from the Late Antique Site of Son Peretó (Mallorca, Balearic Islands, Spain): Archaeological Implications. *Archaeometry* 55 (6): 1101-1121.

Murrieta, P.A., Wheatley, D.W., Strutt, K., Mas Florit, C. and Cau, M.A. 2012. Resultados preliminares de la prospección geofísica en la basílica de Fornells (Mercadal, Menorca). *Revista de Menorca* 91: 59-82.

Neubauer, W., Eder-Hinterleitner, A. 1997. 3D-interpretation of postprocessed archaeological magnetic prospection data. *Archaeological Prospection 4* (4): 191–205.

Neubauer, W. and Eder-Hinterleitner, A. 1997. Resistivity and magnetics of the Roman town Carnuntum, Austria: an example of combined interpretation of prospection data. *Archaeological Prospection*, *4*(4), 179-189.

Palol, P. de, 1967. *Arqueología cristiana de España romana. Siglos IV-VI*, Consejo Superior de Investigaciones Científicas: Madrid.

Palol, P. de, Alomar, A., Camps, J., Rosselló, G., 1967. Notas sobre las basílicas de Manacor en Mallorca. *Boletín del Seminario de Arte y Arqueología,* 33: 1-45.

Ramos-Guerrero, E., I. Berrio, J. Fornos, J., Moragues, L. 2000. The middle Miocene Son Verdera lacustrine-palustrine system (Santa Margalida Basin, Mallorca). In Lake basins through space and time, E. H. Gierlowski-Kordesch and K. R. Kelts (eds.). AAPG Studies in Geology 46, 441-448.

Schmidt, A. 2009. Electrical and magnetic methods in archaeological prospection. In *Seeing the unseen. Geophysics and Landscape Archaeology*, S. Campana, S. Piro (eds.). Taylor & Francis Group: London, 67-82.

Schmidt, A., Tsetskhladze, G. 2013. Raster was yesterday: using vector engines to process geophysical data. *Archaeological Prospection, 20* (1), 59-65.

Tsokas, G. N., Stampolidis, A., Mertzanidis, I., Tsourlos, P., Hamza, R., Chrisafis, C., Ambonis, D., Tavlakis, I. 2007. Geophysical Exploration in the Church of Protaton at Karyes of Mount Athos (Holy Mountain) in Northern Greece. *Archaeological Prospection* 14: 75–86.

Verdonck, L. 2012. High-resolution ground-penetrating radar prospection with a modular configuration, Ghent University, PhD dissertation.

Ulbert, T. 2003. El yacimiento paleocristiano de Son Fadrinet (Campos, Mallorca), Mayurqa 29: 173-187.

Zöllner, H., Kniess, R., Meyer, C. Trinks, I. 2011. Efficient large-scale magnetic prospection using multi-channel fluxgate arrays and the new digitizer LEA D2. In *Archaeological Prospection 9thInternational Conference*, Drahor, M.G., Berge M.A. (eds.). Archaeology and Art Publications: Turkey, 21-23.

Figure Captions

1. Map of Mallorca and the location of Son Peretó, and aerial photograph of the early Christian Complex with indication of the main areas cited in the text.

2. The topography of the site and the areas of investigation. A) Contour lines of the site and the location of the basilica. B) Survey areas by method.

3.GPR data interpretation parameters. Examples of features detected in the survey as seen in single GPR profiles.

4. Results of the magnetic investigation displayed in greyscale values of ±5 nT/m.

5. Interpretation of the magnetic investigation.

6. Results of the GPR survey inside the remains of the basilica, including two single profiles crossing anomaly Groups 72, 78, 83 and 84 Lower-right image: IDS GPR system used in the surveys.

7. GPR results obtained in the surrounding areas of the excavated remains of the basilica complex. Grids 0, G2 and G3.

8. GPR results southeast of the basilica complex (Grid 9).

9. GPR results on the central region, including Grids 8, 5 and G1.

10. Interpretation diagram of Grid G1 and single GPR profiles of located cavities

11. GPR results on the south-west region, including Grids G4, 6 and 7

12. Complementary character of the magnetic and GPR data. A and B show the magnetic map and the interpretation diagram. B and C show the GPR vectorial anomaly map and the synthetic interpretation.

Table captions

Table 1. Technical conditions of the magnetic survey

Table 2. Technical condition of the GPR survey

Table 3. Archaeological site of Son Peretó, general information

Method	**Magnetic prospection**
System	LEA MAX (Eastern Atlas)
Sensors	7 Förster Fluxgate Gradiometer FEREX CON650
Data logger	LEA D2 with 10 channels (Eastern Atlas)
Measurement category	Vertical gradient in nT
Configuration	7 sensors, mounted on cart Vertical sensor separation: 0.65 m
Resolution	0.5 m profile distance max. 0.1 m point distance
Topographic measurement	2x SMART V1 GNSS receiver (with embedded NovAtel OEM6 technology)
Data positioning	Relative error: 0.02
Processing and filters	Eastern Atlas decoding program including offset and drift correction
Data format	ASCII, GeoTiff
Image resolution	0.1 m x 0.1 m

Table 1

Method	GPR prospection		
System	IDS Fast-wave custom 5-antenna system		
Sensors	IDS 5X600MHz		
Data logger	Panasonic CF-18		
Measurement category	Amplitudes (SI)		
Configuration	5 antennas separated 0.20 m		
	600 MHz	60 ns	512 samples per trace
Resolution	0.20 m between profiles; 0.027 m between traces		
Data positioning	Integrated encoder and local coordinates with subsequent georeferencing.		
Topographic measurement	3 points of the local system were measured using a DGPS (EPSG 25831)		
Processing and filters	Drift correction (based on 24-28 average samples), background, time slicing		
Data format	ASCII, GeoTiff, .grd		
Image resolution	0.1 m x 0.1 m		

Table 2

Site	**Son Peretó**
Historical context	Roman and Late Antiquity
Terrain	Flat to very steep
Geology	Miocenic and Pleistocenic marès (biocalcarenite)
Soil	Sand, silt, partly organically enriched
Surface	Mostly even, plough marks
Above ground archaeological features	Archaeological excavation, fragments of pottery and building material
Vegetation	Grass, a few trees
Land use	Harvested crops, uncultivated grass land
Weather	Max. 33°C, sunny, dry
Sources of disturbance	Fences, few scrap metal
Investigated area	Approx. 7.75 ha (Magnetic prospection), 1.958 ha (GPR)

Table 3

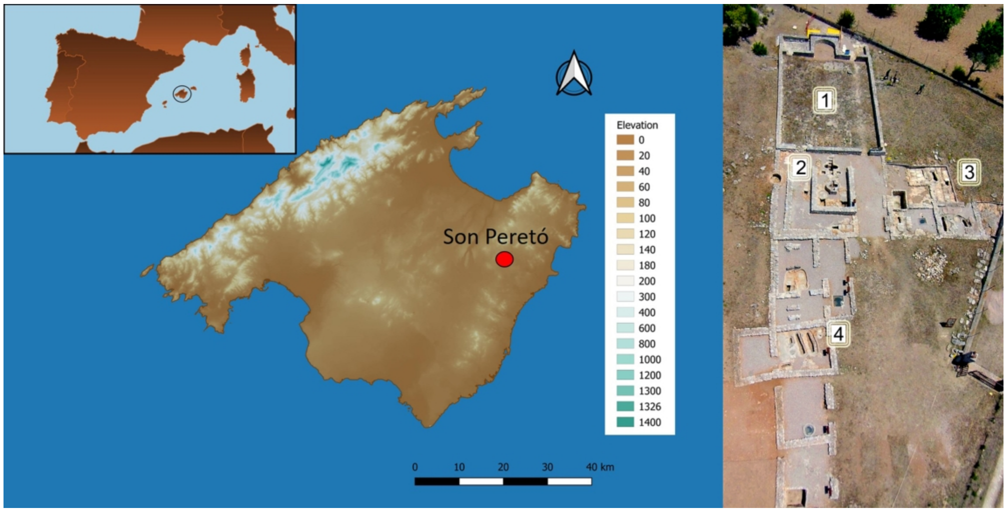

Map of Mallorca and the location of Son Peretó, and aerial photograph of the early Christian Complex with indication of the main areas cited in the text.

169x85mm (300 x 300 DPI)

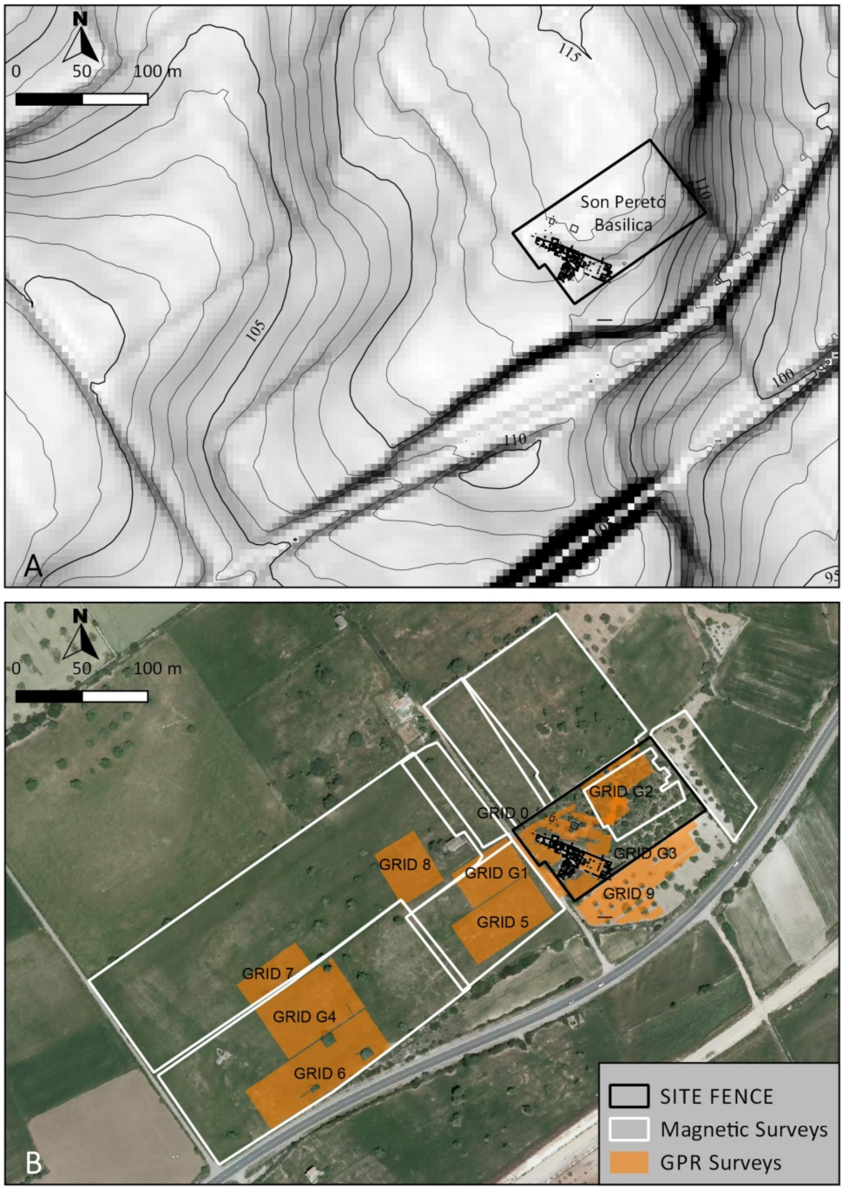

The topography of the site and the areas of investigation. A) Contour lines of the site and the location of the basilica. B) Survey areas by method.

154x216mm (300 x 300 DPI)

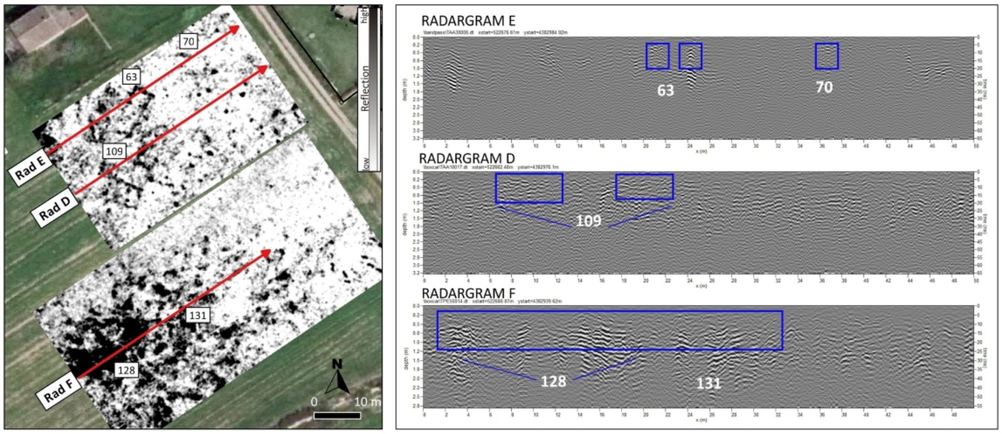

GPR data interpretation parameters. Examples of features detected in the survey as seen in single GPR profiles.

308x133mm (300 x 300 DPI)

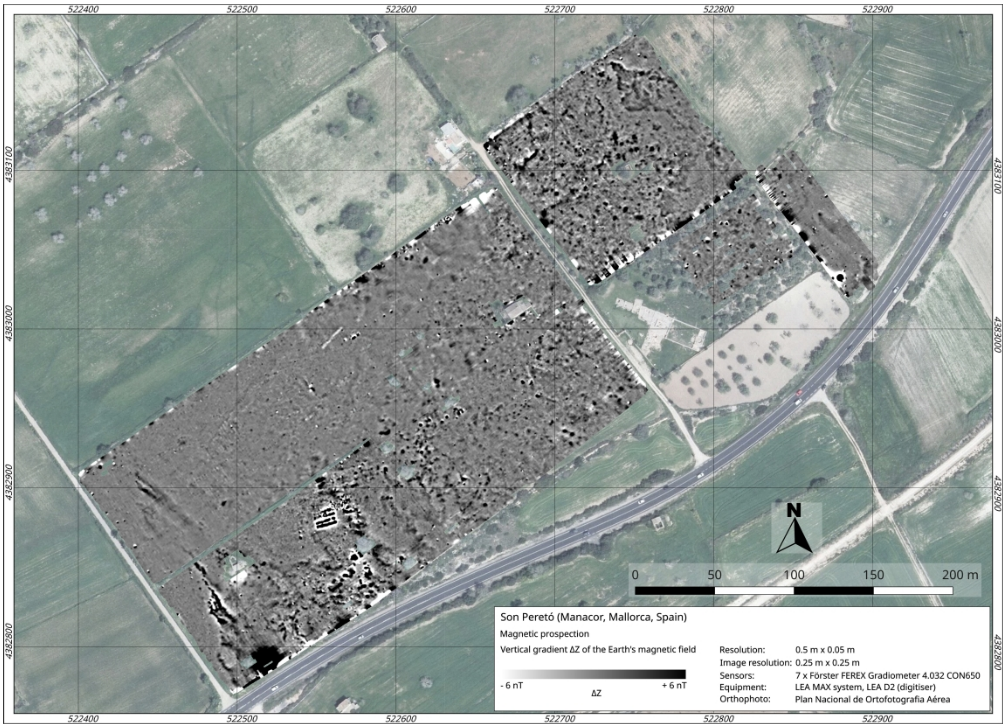

Results of the magnetic investigation displayed in greyscale values of ±5 nT/m.

421x303mm (299 x 299 DPI)

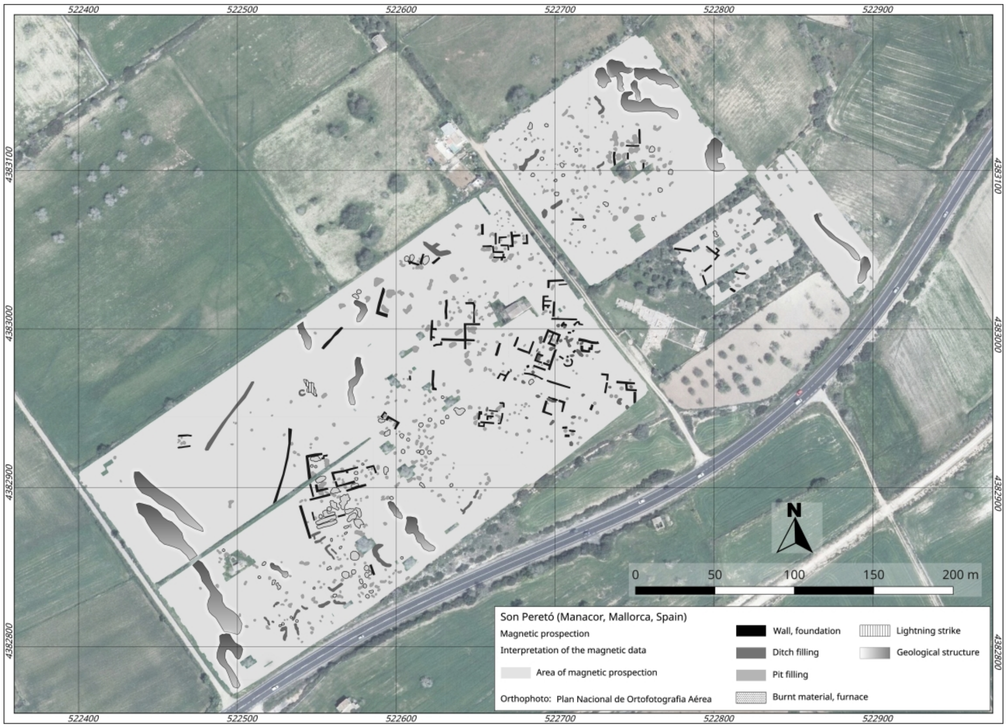

Interpretation of the magnetic investigation.

421x303mm (299 x 299 DPI)

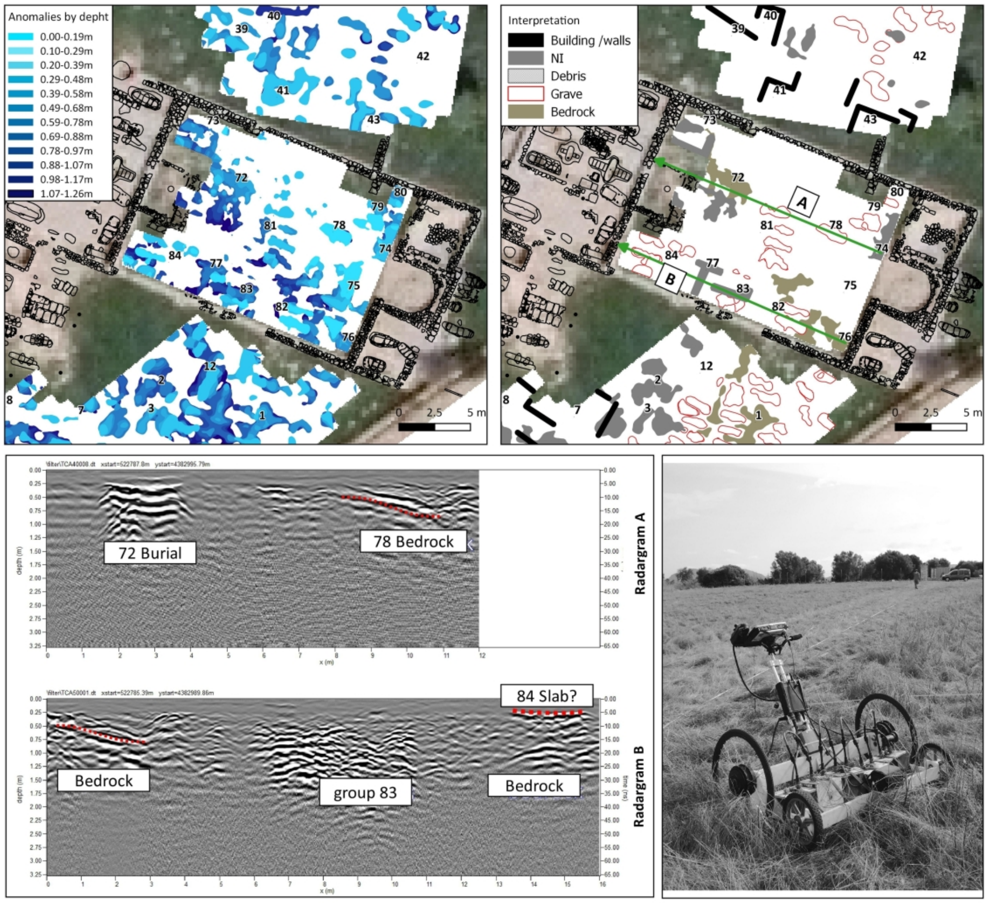

Results of the GPR survey inside the remains of the basilica, including two single profiles crossing anomaly Groups 72, 78, 83 and 84 Lower-right image: IDS GPR system used in the surveys.

279x254mm (300 x 300 DPI)

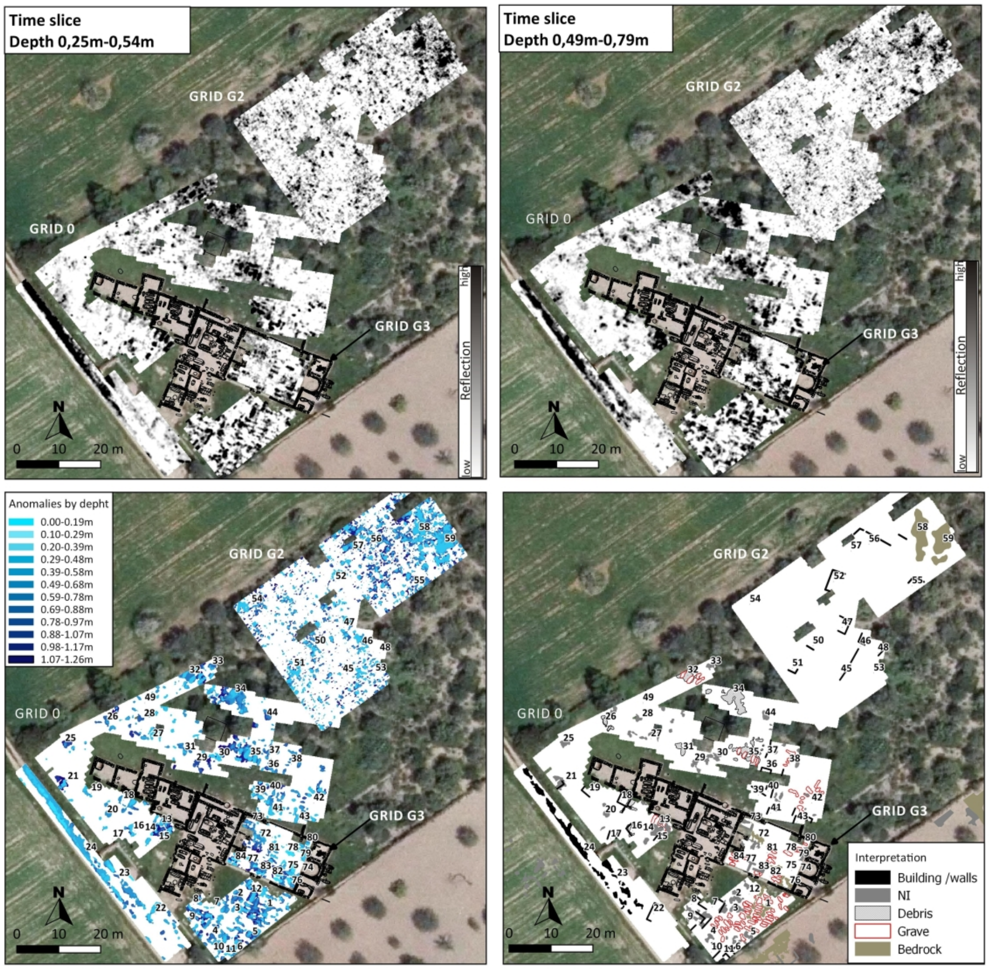

GPR results obtained in the surrounding areas of the excavated remains of the basilica complex. Grids 0, G2 and G3.

279x273mm (300 x 300 DPI)

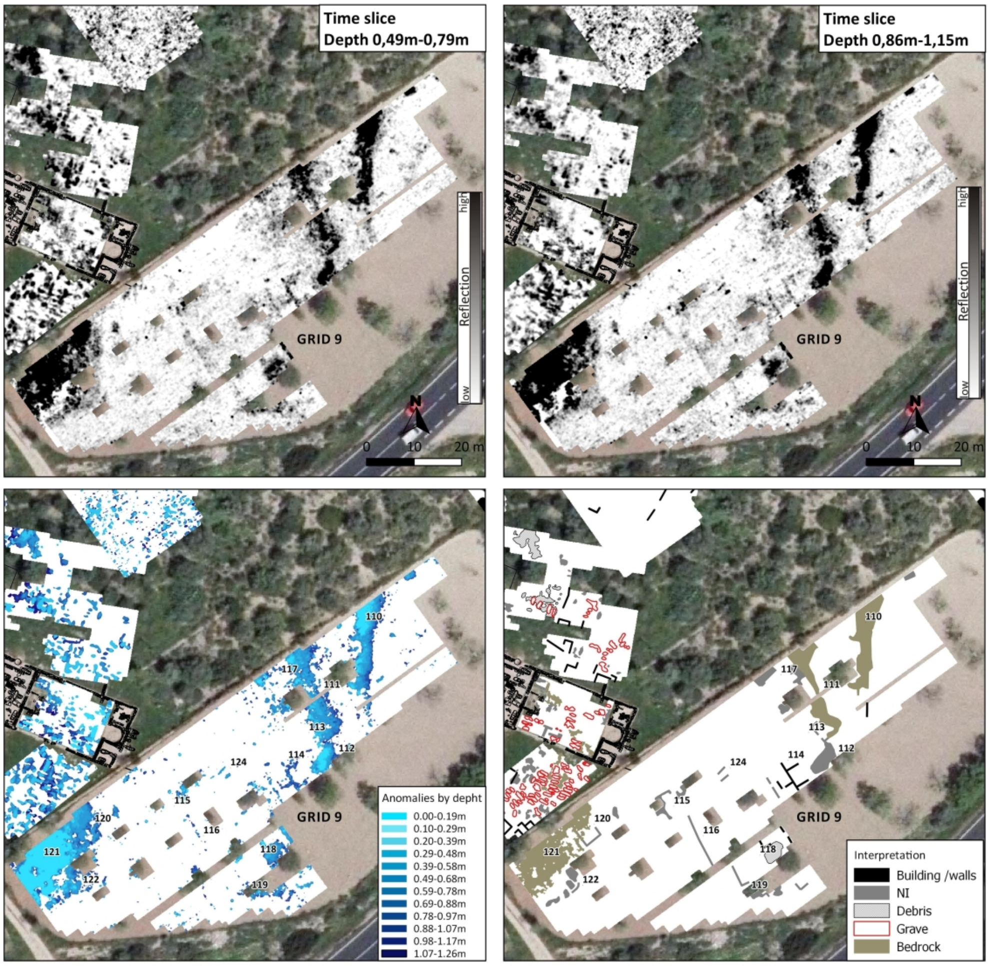

GPR results southeast of the basilica complex (Grid 9).

279x273mm (300 x 300 DPI)

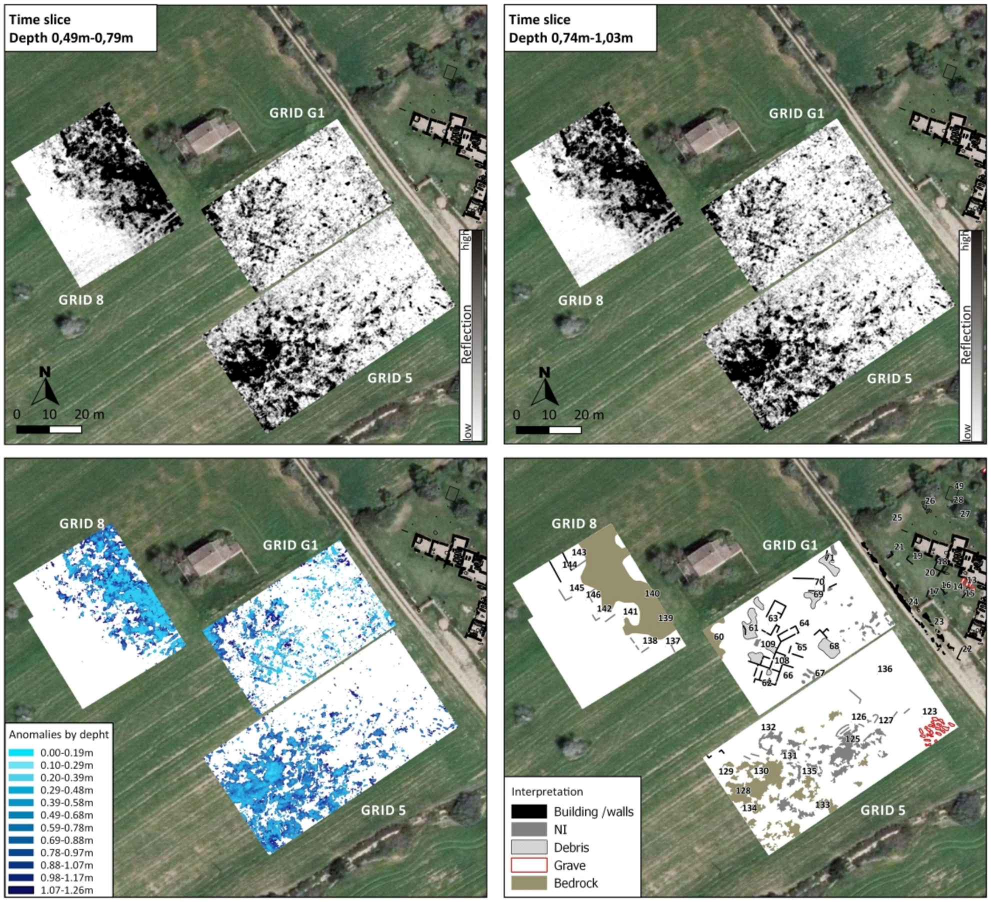

GPR results on the central region, including Grids 8, 5 and G1.

279x254mm (300 x 300 DPI)

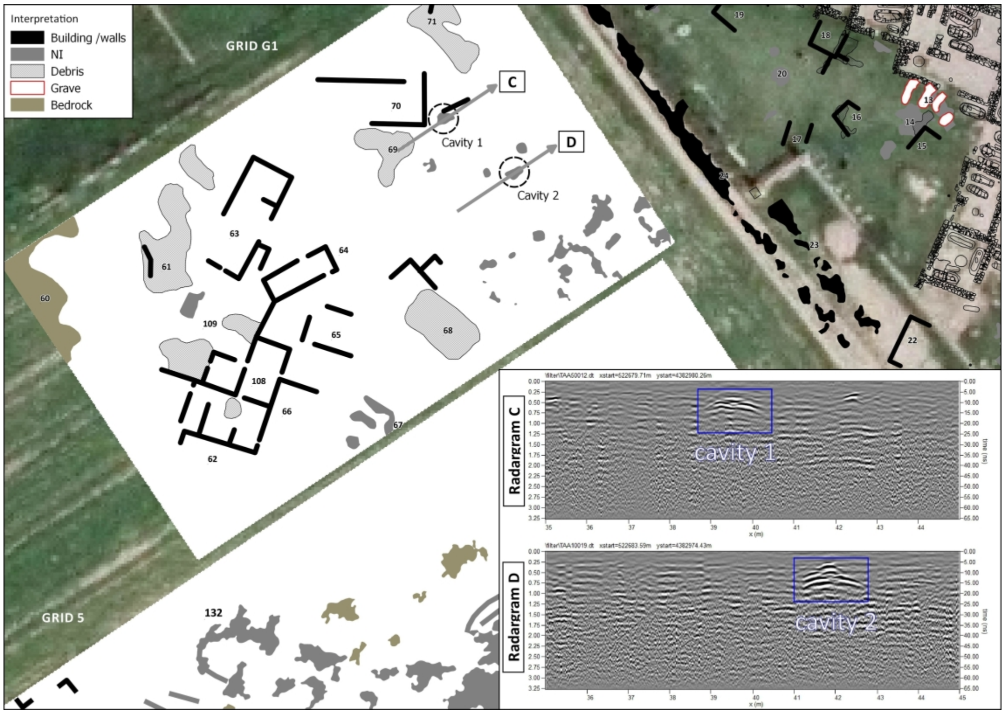

Interpretation diagram of Grid G1 and single GPR profiles of located cavities.

296x209mm (300 x 300 DPI)

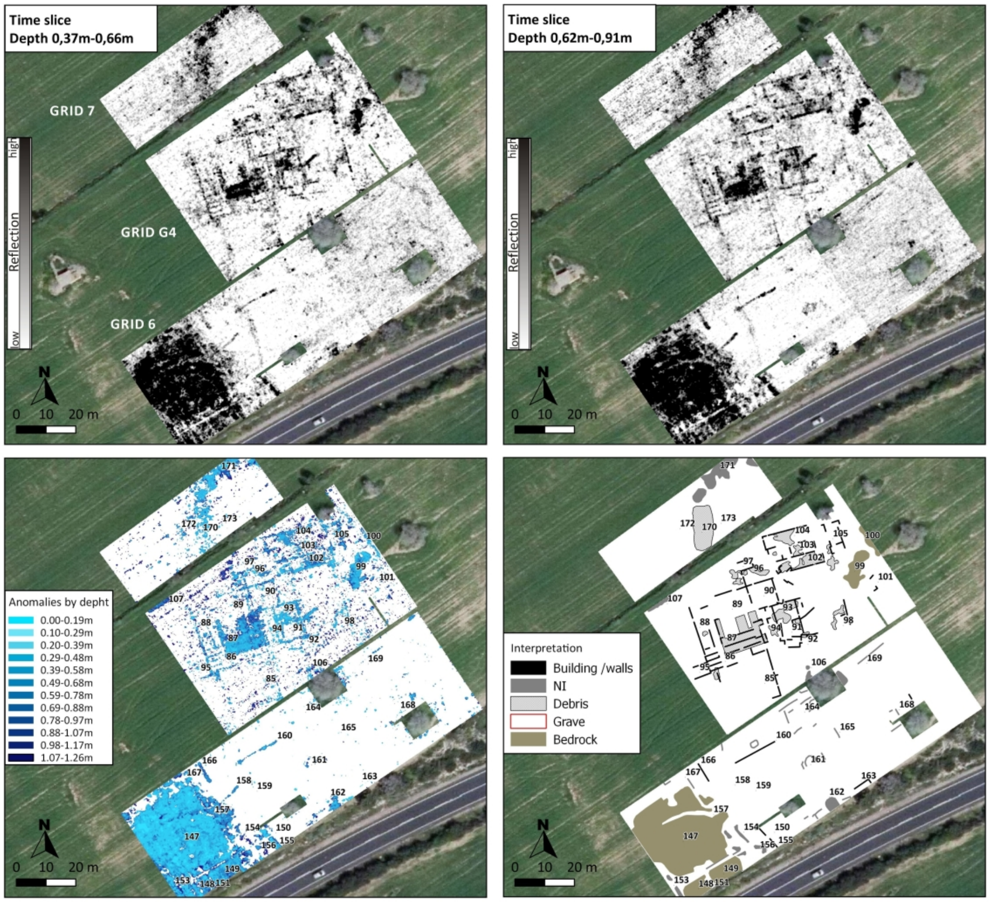

GPR results on the south-west region, including Grids G4, 6 and 7.

279x254mm (300 x 300 DPI)

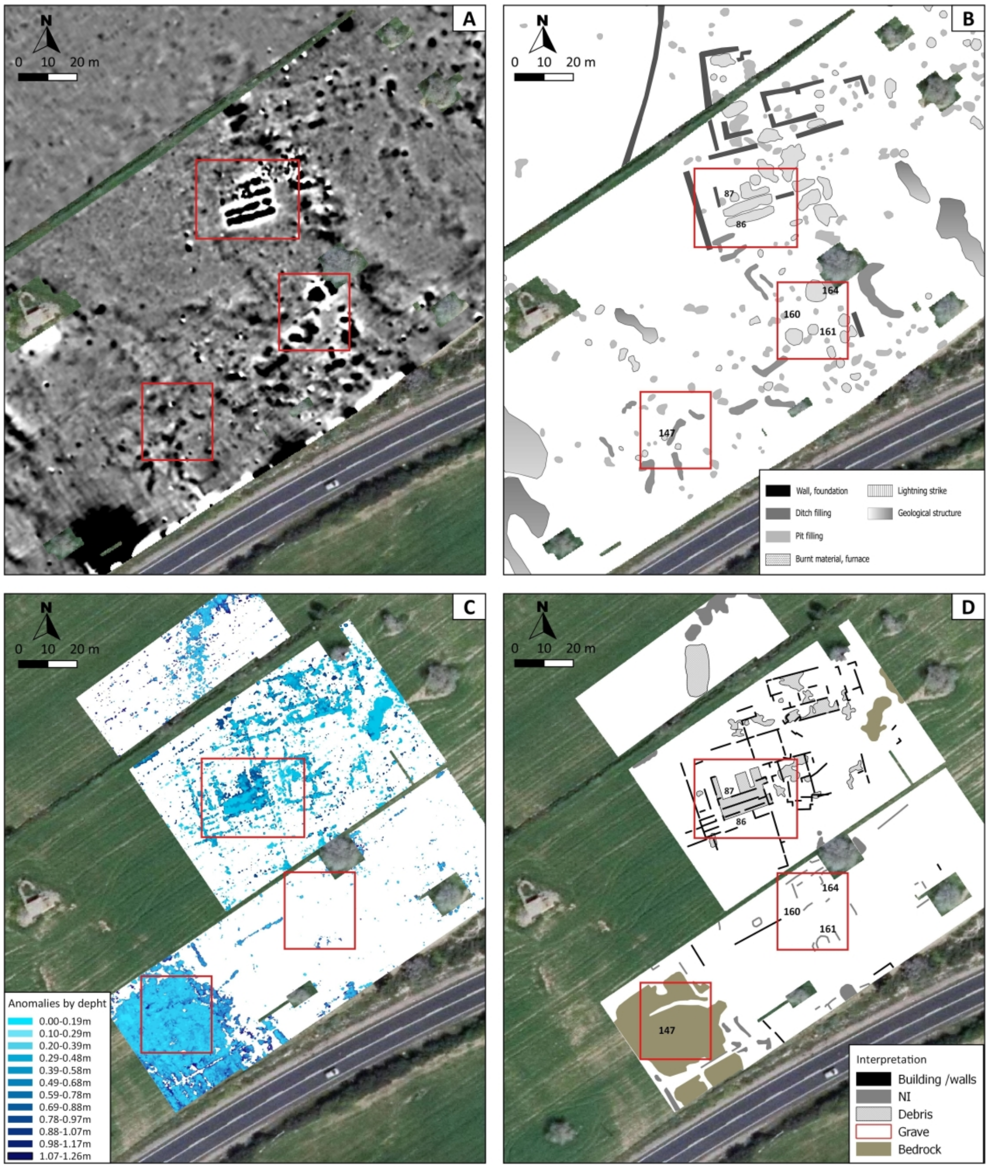

Complementary character of the magnetic and GPR data. A and B show the magnetic map and the interpretation diagram. B and C show the GPR vectorial anomaly map and the synthetic interpretation.

284x333mm (300 x 300 DPI)